Myocardial Microstructure and Contractile Apparatus

Umamah Tarvala and Zohya Khalique

What You Will Learn in This Chapter

This chapter will address the anatomy of the heart from a microstructural perspective and review how the organisation of cardiomyocytes supports cardiac function. Both the helical arrangement of cardiomyocytes and the orientation of sheetlets will be examined. The potential of a novel technique called diffusion tensor cardiovascular magnetic resonance (DT-CMR) will be discussed, in particular its ability to non-invasively assess the cardiac microstructure in both health and disease.

4

Learning Objectives

- Acknowledge the complexity of the myocardial microstructure.
- Understand how the configuration of cardiomyocytes and sheetlets relate to ventricular contractile function.
- Appreciate how novel non-invasive techniques will aid our understanding of the dynamics of the myocardial microstructure.

4.1 Cardiac Microstructure

The cardiac microstructure is complex, and its dynamics are not yet fully understood. It is often considered to have a hierarchical structure. Sarcomeres are the basic contractile units of the myocardium and are aligned in series to form myofibrils, which themselves assemble within the cardiomyocytes (CMs) in parallel. CMs connect end to end with several others in a branching configuration [1]. Moreover, CMs aggregate into secondary structures called *sheetlets* that underlie the laminar nature of the myocardium [2, 3]. There is an important relationship between the microstructure and overall cardiac function.

4.1.1 Sarcomeres

Sarcomeres are formed of thin and thick filaments and are approximately 2 μm long. They are bounded by Z-discs [4]. The thin filament comprises actin molecules associated with the troponin complex (troponins T, I and C) and tropomyosin. Tropomyosin rests over the myosin-binding site of the actin filament [5]. The thick filament comprises two myosin heavy chains and four myosin light chains. In each thick filament, there are three key regions: the motor head, the hinge at the neck and the tail.

The arrangement of the filaments gives rise to alternating light (I) and dark (A) bands [4]. The lighter I bands contain only the thin filament, whilst the darker A band includes the thick filament as well as the area of overlap with the thin filament. The A band also contains the H zone, a region of no actin. The M line reflects the centre of the sarcomere, with the protein *titin* running from the M line to the Z disc.

4.1.2 Cardiomyocytes

CMs are multinucleated cells, with a principal long axis and multiple intercalations with other CMs. There is a surprising lack of agreement in the terminology relating to CM organisation, with the term 'fibre' being used to describe both individual CMs and groups of CMs [6]. Others avoid the term altogether to retain the distinction between cardiac and skeletal muscle.
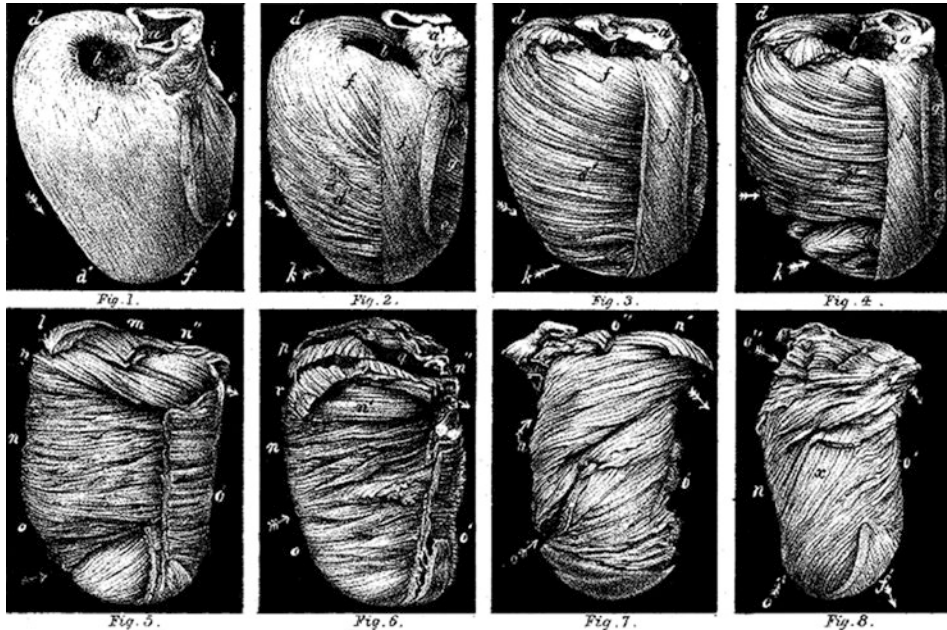
Fig. 4.1   The left ventricle (LV) has a helical arrangement. The LV is dissected from the epicardium (top left) through several layers to the endocardium (bottom right). There is transmural variation in the orientation of the cardiomyocytes. (Image from [7])

Gross dissection of mammalian hearts reveals a 'grain-like' appearance to the myocardium, reflecting the overall direction of CM long axis orientation [7]. The CMs have a helical orientation, as shown in ◘ Fig. 4.1. In the epicardium, CMs are orientated in a negative left-handed (LH) helix, rotated through to a circumferential alignment in the mesocardium and progress to a positive right-handed (RH) helix in the endocardium. Both light [8] and extended volume confocal microscopy [9] techniques confirm this transmural variation of the cardiomyocyte orientation from approximately −70° at the epicardium to +70° at the endocardium (where the angle lies between the CM long axis and the circumferential direction and is projected onto the plane tangential to the epicardium).

4.1.3   Sheetlets

A secondary level of CM organisation exists, in which groups of approximately 8–12 CMs aggregate, surrounded by collagenous perimysium and separated by shear layers [2, 3]. These grouped CMs are termed sheetlets, shown in ◘ Fig. 4.2. Originally, it was believed that sheetlets spanned the entire width of the LV wall; however, it is now appreciated that there are multiple sub-populations of sheetlets with differing orientations throughout the LV [11–13].

An important collagenous network exists, interlaced with the CMs and sheetlets. In the subepicardium, long interconnected cords of collagen run parallel to the long axis of CMs. In the mid-wall, perimysial collagen surrounds sheetlets, forming part of the cleavage planes that are seen in ◘ Fig. 4.2. Longitudinal cords (base-apex) are less frequently

Fig. 4.2 Histology of porcine myocardium from the mid-left ventricular wall. Cardiomyocytes are seen in cross section and aggregate into groups, separated by the white fissures or 'shear layers'. (Adapted from [10])
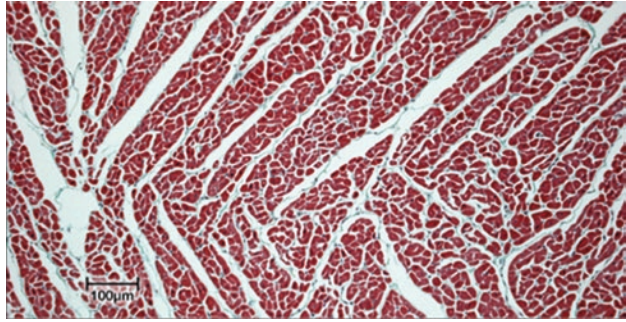
observed in the mesocardium. In the subendocardium, there is a dominance of the cleavage plane structure in the collagen network, suggesting that the sheetlet configuration is increasingly well-defined towards the endocardium [2]. These cleavage planes are not simply space between sheetlets or distortion artefacts from histological preparation, but in fact play an important role in the dynamic nature of the myocardium.

4.2 Structure–Function Relationship

Cardiac function is complex, with multidirectional myocardial deformations occurring across the cardiac cycle. The interplay of radial thickening and thinning, longitudinal and circumferential shortening, lengthening, and torsion all contribute to LV function. Whilst ejection fraction (EF) is the most ubiquitous of parameters used to define contractile function, it measures luminal change, rather than myocardial mechanics directly. *Strain* is a measure of myocardial deformation (relative change from resting diastolic dimension) and is typically described by dimensionless units. Global longitudinal strain has been shown to be superior to EF in predicting major adverse cardiac events [14].

Radial strain reflects LV wall thickening and is positive, typically in the range of 0.40. In contrast, circumferential and longitudinal strain are both negative, and approximately −0.20 [15, 16]. These strains are in the direction of the normal orthogonal directions, but more complex cross-directional deformations known as shear also exist.

4.2.1 Sarcomeric Function

These various strains are underpinned by the contractile force generated by the sarcomere. It is the dynamic interaction of the thick and thin filament that produces contractile force. This is known as the '*sliding filament theory*' [4, 17]. CM membrane depolarisation results in the release of Ca^{2+} from the sarcoplasmic reticulum, which binds to troponin C. This, as well as phosphorylation of troponin I results in tropomyosin rotating around the actin filament and opening the myosin binding site [5, 18]. Consequently, the myosin head is able to form a crossbridge with the actin filament and slide it along towards the centre of the A band in a 'power stroke'. Adenosine triphosphate (ATP) then binds to the myosin head, and the crossbridge detaches.

Sarcomere length reduces in systole to approximately 80–65% of its diastolic length, due to this sliding filament motion. It is recognised that there is a length–tension

relationship of increasing force generation as diastolic sarcomere length increases. This accords with the ascending limb of the Frank-Starling law curve; increasing contractility (cardiac output) as diastolic filling (end-diastolic volume) rises. This will be explained further in ▶ Chap. 10 [19].

4.2.2 Relating Cardiomyocytes to Cardiac Function

There is an intuitive relationship between sarcomeric shortening of ~15% and CM shortening of a similar magnitude. Indeed, this value approximates to the negative circumferential strain seen in the mid-wall where CMs are circumferentially aligned [17, 20]. What is less clear is how the associated ~8% CM thickening translates into wall thickening of 40% – a paradox addressed by many groups over recent decades [8, 21–23].

Initially, it was recognised that cleavage plane orientation differed in different contractile states, supporting the concept of redistribution of myocardial volume through the cardiac cycle [21]. The identification of sheetlets, married with experiments measuring shear strains, developed the subsequent explanation of sheetlets sliding relative to one another, facilitating wall thickening beyond individual CM thickening [22–24]. However, such shear analyses do not directly assess sheetlet orientation, with these studies further limited by the static nature of histology.

Recent novel developments in a technique called *diffusion tensor cardiovascular magnetic resonance* (DT-CMR) have been instrumental in developing our understanding of this conundrum [25]. DT-CMR is a unique non-invasive tool that can evaluate the cardiac microstructure in vivo by probing the diffusion of water through the myocardium. Both the mean CM long axis orientation and the dominant sheetlet direction can be obtained, as demonstrated in ◨ Fig. 4.3 [26–28]. The technique has been histologically validated through various experiments, including in vivo, in situ, ex vivo and histological correlation [26, 28–31]. It has been applied in humans to give dynamic information about the microstructural rearrangements that are integral to wall thickening and LV contraction [26]. In diastole, sheetlets are orientated parallel to the LV epicardial wall; however, in systole they reorient to a more wall-perpendicular alignment, facilitated by the shear layers. This degree of reorientation is referred to as *sheetlet mobility*.

Interestingly, the helix angle does not undergo substantial change between diastole and systole, instead retaining the negative-to-positive helix angle progression that appears to be preserved throughout the mammalian species [7, 26]. Rather, the helical arrangement is key in driving myocardial rotation and torsion [32]. CM shortening of the LH epicardial myocytes leads to clockwise rotation basally and anticlockwise rotation apically, when viewed from the apex. Contraction of the RH subendocardial myocytes results in anticlockwise rotation basally and clockwise rotation apically. There is a net clockwise rotation basally and anticlockwise rotation apically, due to the dominant effect of the larger epicardial radius [33].

These opposing rotations give rise to LV torsion – the wringing effect that aids effective LV emptying. The consequent recoil in diastole facilitates passive LV filling [34]. Hence, there is an important relationship between the helical arrangement of cardiomyocytes and LV function.
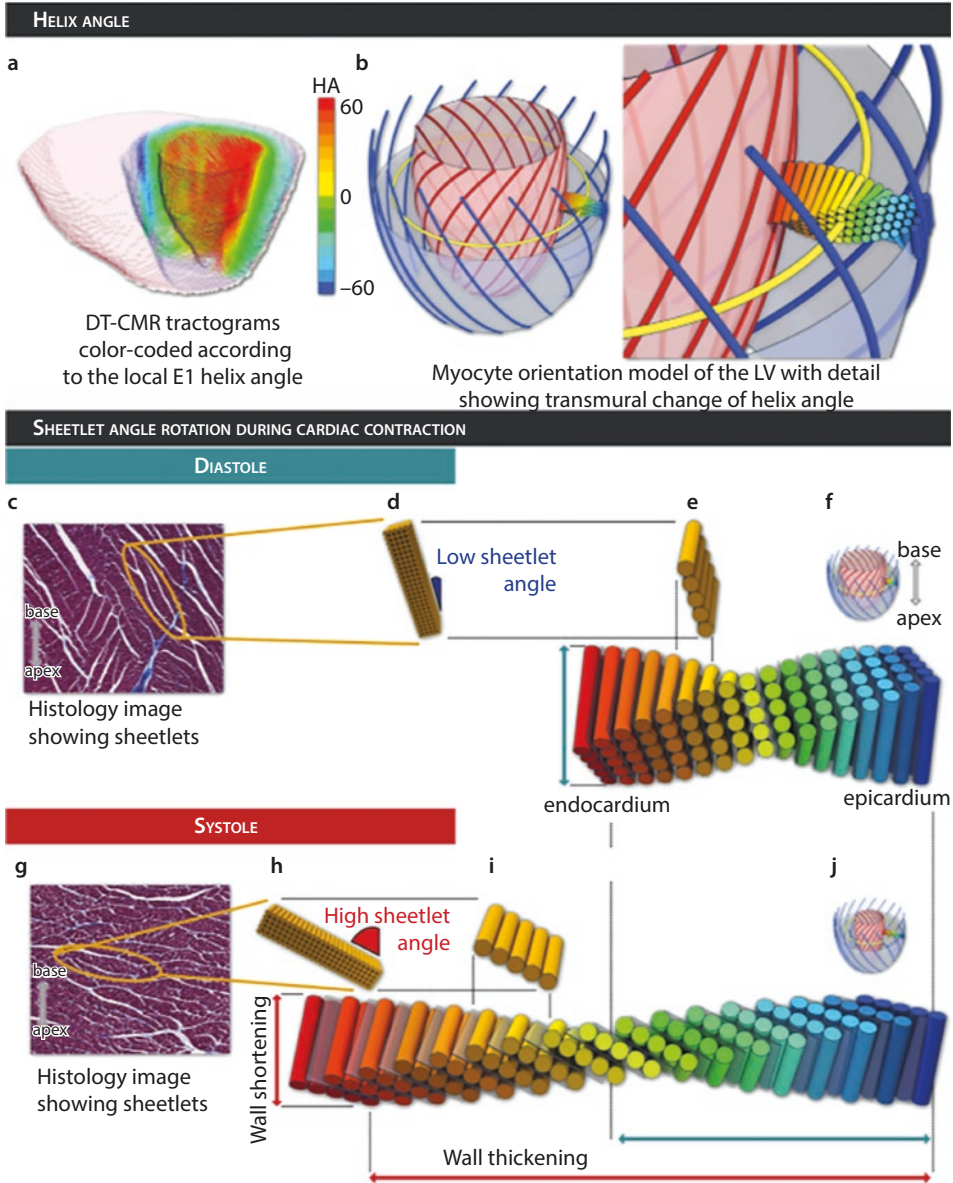
4

HELIX ANGLE

a

b

DT-CMR tractograms color-coded according to the local E1 helix angle

Myocyte orientation model of the LV with detail showing transmural change of helix angle

SHEETLET ANGLE ROTATION DURING CARDIAC CONTRACTION

DIASTOLE

c   **d**   **e**   **f**

Low sheetlet angle

base

apex

Histology image showing sheetlets

endocardium   epicardium

SYSTOLE

g   **h**   **i**   **j**

High sheetlet angle

Histology image showing sheetlets

Wall shortening

Wall thickening

Fig. 4.3   DT-CMR provides cardiomyocyte and sheetlet orientation. In the top row, helix angle (HA) is depicted. DT-CMR tractography demonstrates the known transmural variation from a negative HA at the epicardium (blue) through to a positive HA in the endocardium (red). In the bottom panel, the sheetlet angle is demonstrated with porcine histology alongside. In diastole, histology (**c**) shows a more wall-parallel sheetlet orientation, which is a low sheetlet angle (**d**–**f**). In systole, a more wall-perpendicular orientation occurs, shown in histology (**g**), which translates to a higher sheetlet angle (**h, I**). While cardiomyocyte orientation remains similar in both cardiac phases, there is a significant increment in sheetlet angle, which marries with the increased wall thickness (**j**). (Image from [26])

4.3 Clinical Implications: DT-CMR in Microstructural Derangement

DT-CMR is the only tool that allows for the non-invasive in vivo characterisation of the myocardial microstructure. It has offered novel insight into our understanding of myocardial mechanics in health, but also in disease. In acute myocardial infarction, the proportion of RH helical structures decreases, concordant with the susceptibility of the endocardium to ischaemia. Subsequent to this, a gain of LH cardiomyocytes in the infarct zone and RH cardiomyocytes in the remote zone are thought to be adaptive remodelling responses [35, 36]. Disturbance of the microarchitecture post-infarct has been characterised by DT-CMR, which may offer a contrast-free method of delineating cardiac fibrosis, in addition to identifying a potential new tool to guide catheter ablation procedures for infarct-driven ventricular arrhythmias [37].

DT-CMR has also identified novel abnormalities in sheetlet behaviour in cardiomyopathy. In hypertrophic cardiomyopathy (HCM), sheetlets have been demonstrated as retaining a more systolic-like orientation (more wall-perpendicular) in diastole, with reduced sheetlet mobility [10, 26]. The failure of sheetlets to return to a more wall-parallel orientation in diastole can be described as a 'failure of diastolic relaxation'. Interestingly, this microstructural abnormality builds upon our knowledge of HCM pathophysiology. Many sarcomeric mutations result in increased myofilament sensitivity to calcium, increasing relative CM tension and contributing to the diastolic dysfunction in HCM [38, 39]. In contrast, sheetlets in dilated cardiomyopathy (DCM) have been observed as failing to re-align to the expected systolic wall-perpendicular angulation, instead retaining a more diastolic-like configuration [26].

In both of these cardiomyopathies, radial strain is similarly reduced; however, DT-CMR is able to identify the respective sheetlet abnormalities, providing a deeper understanding of the pathophysiology underlying the diseases. HCM and other forms of cardiomyopathy will be expanded upon in greater detail in ▶ Chap. 12.

In congenital heart disease, DT-CMR of patients with situs inversus totalis has disproven the idea that the condition is one of simply gross positional abnormality. Instead, gross derangement of the helical arrangement was demonstrated, with an inverted pattern basally that transitions to a more solitus pattern apically (◼ Fig. 4.4). In the mid-ventricular transition zone, decreased sheetlet mobility and strain were identified, whilst overall absolute torsion was reduced [40].

4.4 Where We're Heading

Our understanding of the cardiac microstructure and its relationship with cardiac function continues to grow. Novel tools such as DT-CMR are critical to developing our appreciation of this complex interplay. Whilst the sheetlets and their dynamics during the cardiac cycle can be demonstrated in vivo, it is unclear whether wall thickening results from microstructural rearrangement or vice versa. In the same vein, does impaired sheetlet mobility reflect or drive the cardiomyopathic process? There are inherent differences in the morphology of the right and left ventricles and so the microstructural assessment of both ventricles needs further study.
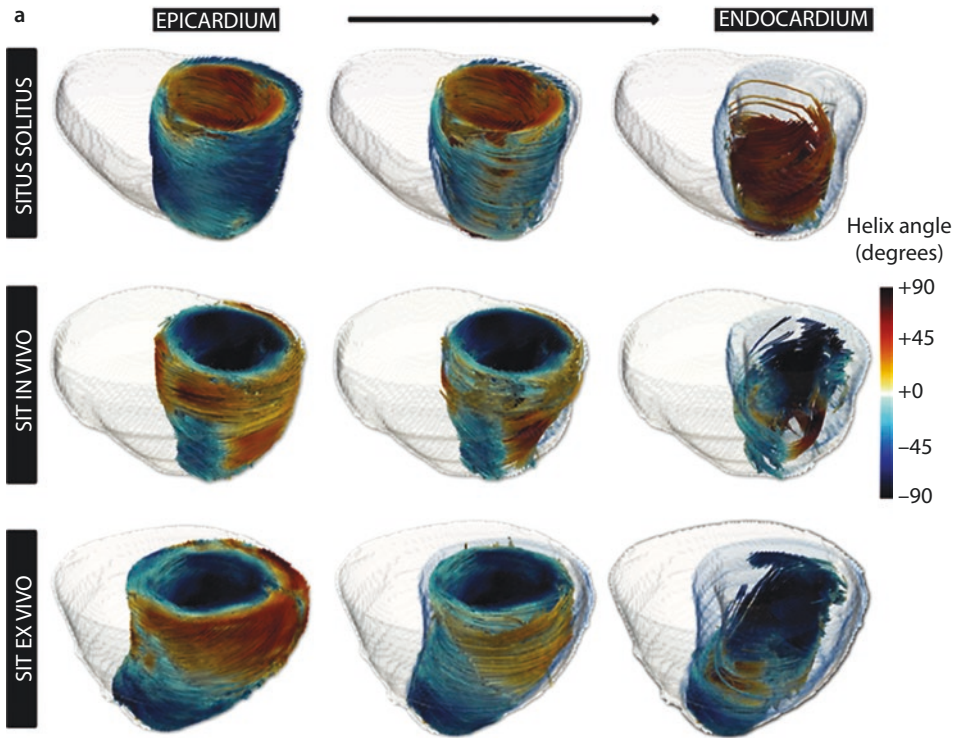
4

a

EPICARDIUM → ENDOCARDIUM

SITUS SOLITUS

SIT IN VIVO

SIT EX VIVO

Helix angle (degrees)

+90
+45
+0
−45
−90

🔲 **Fig. 4.4** CM orientation is deranged in situs inversus. DT-CMR demonstrates the expected helical arrangement in situs solitus, whereby CM orientation progresses from a negative helix (blue) at the epicardium towards a positive helix angle (red) at the endocardium. Neither the in-vivo and ex-vivo situs inversus hearts exhibit this profile and instead show inversion at the base that trends towards the situs solitus arrangement at the apex. There is a mid-ventricular transition zone. Adapted from [40]

Take-Home Message

- The myocardial microstructure is complex, with multiple levels of organisation. Cardiac function is more than the ejection fraction. Various myocardial deformations take place through the cardiac cycle, including radial thickening, circumferential and longitudinal shortening, as well as torsion.
- Cardiomyocytes have a helical arrangement that transitions from left-handed in the epicardium through circumferential in the mesocardium and right-handed in the endocardium. This organisation is typically preserved in mammals and drives cardiac torsion.
- A second level of cardiomyocyte organisation exists, in which aggregated cardiomyocytes form sheetlets. These sheetlets re-orientate through the cardiac cycle and are integral to the process of wall thickening.
- DT-CMR is a novel tool that can non-invasively offer information about cardiomyocyte and sheetlet orientations in vivo. It has identified sheetlet abnormalities in cardiomyopathy, deranged cardiomyocyte structure in congenital heart disease and can assess microarchitectural changes following myocardial infarction.

References

1. Braunwald E, Ross J, Sonnenblick EH (1967) Mechanisms of contraction of the normal and failing heart. N Engl J Med 277:910
2. Pope AJ, Sands GB, Smaill BH, LeGrice IJ (2008) Three-dimensional transmural organization of perimysial collagen in the heart. AJP Hear Circ Physiol. 295:H1243
3. LeGrice I, Smaill B, Chai L, Edgar S, Gavin J, Hunter P (1995) Laminar structure of the heart: ventricular myocyte arrangement and connective tissue architecture in the dog. Am J Physiol Heart Circ Physiol 269:H571
4. Huxley AF, Niedergerke R (1954) Structural changes in muscle during contraction: interference microscopy of living muscle fibres. Nature 173(4412):971–973
5. Lehman W, Craig R, Vibert P (1994) Ca2+-induced tropomyosin movement in Limulus thin filaments revealed by three-dimensional reconstruction. Nature 368(6466):65–67
6. Gilbert SH, Benson AP, Li P, Holden AV (2007) Regional localisation of left ventricular sheet structure: integration with current models of cardiac fibre, sheet and band structure. Eur J Cardiothorac Surg 32:231
7. Pettigrew JB (1864) On the arrangement of the muscular fibres in the ventricles of the vertebrate heart, with physiological remarks. Philos Trans R Soc Lond 154:445–500
8. Streeter DD, Spotnitz HM, Patel DP, Ross J, Sonnenblick EH (1969) Fiber orientation in the canine left ventricle during diastole and systole. Circ Res 24(3):339–347
9. Sands GB, Smaill BH, LeGrice IJ (2008) Virtual sectioning of cardiac tissue relative to fiber orientation. In: 2008 30th annual international conference of the IEEE engineering in medicine and biology society
10. Ferreira PF, Kilner PJ, Mcgill LA, Nielles-Vallespin S, Scott AD, Ho SY et al (2014) In vivo cardiovascular magnetic resonance diffusion tensor imaging shows evidence of abnormal myocardial laminar orientations and mobility in hypertrophic cardiomyopathy. J Cardiovasc Magn Reson 16:87
11. Helm PA, Younes L, Beg MF, Ennis DB, Leclercq C, Faris OP et al (2006) Evidence of structural remodeling in the dyssynchronous failing heart. Circ Res 98:125
12. Kung GL, Nguyen TC, Itoh A, Skare S, Ingels NB, Miller DC et al (2011) The presence of two local myocardial sheet populations confirmed by diffusion tensor MRI and histological validation. J Magn Reson Imaging 34:1080
13. Harrington KB (2005) Direct measurement of transmural laminar architecture in the anterolateral wall of the ovine left ventricle: new implications for wall thickening mechanics. AJP Hear Circ Physiol. 288(3):H1324–H1330
14. Kalam K, Otahal P, Marwick TH (2014) Prognostic implications of global LV dysfunction: a systematic review and meta-analysis of global longitudinal strain and ejection fraction. Heart 100:1673
15. Moore CC, Lugo-Olivieri CH, McVeigh ER, Zerhouni EA (2000) Three-dimensional systolic strain patterns in the normal human left ventricle: characterization with tagged MR imaging. Radiology 214:453
16. Yingchoncharoen T, Agarwal S, Popović ZB, Marwick TH (2013) Normal ranges of left ventricular strain: a meta-analysis. J Am Soc Echocardiogr 26:185
17. Huxley H, Hanson J (1954) Changes in the cross-striations of muscle during contraction and stretch and their structural interpretation. Nature 173(4412):973–976
18. Layland J, Solaro RJ, Shah AM (2005) Regulation of cardiac contractile function by troponin I phosphorylation. Cardiovasc Res 66:12
19. Fabiato A, Fabiato F (1975) Dependence of the contractile activation of skinned cardiac cells on the sarcomere length. Nature 256:54
20. Sonnenblick EH, Ross J, Covell JW, Spotnitz HM, Spiro D (1967) The ultrastructure of the heart in systole and diastole. Chantes in sarcomere length. Circ Res 21:423
21. Spotnitz HM, Spotnitz WD, Cottrell TS, Spiro D, Sonnenblick EH (1974) Cellular basis for volume related wall thickness changes in the rat left ventricle. J Mol Cell Cardiol 6:317
22. LeGrice IJ, Takayama Y, Covell JW (1995) Transverse shear along myocardial cleavage planes provides a mechanism for normal systolic wall thickening. Circ Res 77:182
23. Cheng A, Nguyen TC, Malinowski M, Daughters GT, Miller DC, Ingels NB (2008) Heterogeneity of left ventricular wall thickening mechanisms. Circulation 118:713
24. Costa KD, Takayama Y, McCulloch AD, Covell JW (1999) Laminar fiber architecture and three-dimensional systolic mechanics in canine ventricular myocardium. Am J Physiol Circ Physiol. 276:H595

4

25. Nielles-Vallespin S, Mekkaoui C, Gatehouse P, Reese TG, Keegan J, Ferreira PF et al (2013) In vivo diffusion tensor MRI of the human heart: reproducibility of breath-hold and navigator-based approaches. Magn Reson Med 70:454
26. Nielles-Vallespin S, Khalique Z, Ferreira PF, de Silva R, Scott AD, Kilner P et al (2017) Assessment of myocardial microstructural dynamics by in vivo diffusion tensor cardiac magnetic resonance. J Am Coll Cardiol 69:661
27. Reese TG, Weisskoff RM, Smith RN, Rosen BR, Dinsmore RE, Wedeen VJ (1995) Imaging myocardial fiber architecture in vivo with magnetic resonance. Magn Reson Med 34:786
28. Scollan DF, Holmes A, Winslow R, Forder J (1998) Histological validation of myocardial microstructure obtained from diffusion tensor magnetic resonance imaging. Am J Physiol Circ Physiol 275:H2308
29. Holmes AA, Scollan DF, Winslow RL (2000) Direct histological validation of diffusion tensor MRI in formaldehyde- fixed myocardium. Magn Reson Med 44:157
30. Hsu EW, Muzikant AL, Matulevicius SA, Penland RC, Henriquez CS (1998) Magnetic resonance myocardial fiber-orientation mapping with direct histological correlation. Am J Physiol Circ Physiol. 274:H1627
31. Chen J (2005) Regional ventricular wall thickening reflects changes in cardiac fiber and sheet structure during contraction: quantification with diffusion tensor MRI. AJP Hear Circ Physiol 289:H1898
32. Rüssel IK, Götte MJW, Bronzwaer JG, Knaapen P, Paulus WJ, van Rossum AC (2009) Left ventricular torsion. An expanding role in the analysis of myocardial dysfunction. JACC Cardiovasc Imaging 2(5):648–655
33. Sengupta PP, Tajik AJ, Chandrasekaran K, Khandheria BK (2008) Twist mechanics of the left ventricle. Principles and application. JACC Cardiovasc Imaging 1(3):366–376
34. Young AA, Cowan BR (2012) Evaluation of left ventricular torsion by cardiovascular magnetic resonance. J Cardiovasc Magn Reson 14:49
35. Wu MT, Su MY, Huang YL, Chiou KR, Yang P, Pan HB et al (2009) Sequential changes of myocardial microstructure in patients postmyocardial infarction by diffusion-tensor cardiac mr correlation with left ventricular structure and function. Circ Cardiovasc Imaging 2:32
36. Wu MT, Tseng WYI, Su MYM, Liu CP, Chiou KR, Wedeen VJ et al (2006) Diffusion tensor magnetic resonance imaging mapping the fiber architecture remodeling in human myocardium after infarction: correlation with viability and wall motion. Circulation 114:1036
37. Mekkaoui C, Jackowski MP, Kostis WJ, Stoeck CT, Thiagalingam A, Reese TG et al (2018) Myocardial scar delineation using diffusion tensor magnetic resonance tractography. J Am Heart Assoc 7(3):e007834
38. Pinto JR, Parvatiyar MS, Jones MA, Liang J, Ackerman MJ, Potter JD (2009) A functional and structural study of troponin C mutations related to hypertrophic cardiomyopathy. J Biol Chem 284:19090
39. Willott RH, Gomes AV, Chang AN, Parvatiyar MS, Pinto JR, Potter JD (2010) Mutations in Troponin that cause HCM, DCM AND RCM: what can we learn about thin filament function? J Mol Cell Cardiol 48:882
40. Khalique Z, Ferreira PF, Scott AD, Nielles-Vallespin S, Kilner PJ, Kutys R et al (2018) Deranged myocyte microstructure in situs inversus totalis demonstrated by diffusion tensor cardiac magnetic resonance. JACC Cardiovasc Imaging 11(9):1360–1362